Fourier Transform Infrared Analysis of Purified Lactose Permease: A Monodisperse Lactose Permease Preparation Is Stably Folded, α-Helical, and Highly Accessible to Deuterium Exchange†

Jason S. Patzlaff,‡,§ Jeffrey A. Moeller,§ Bridgette A. Barry,*,‡ and Robert J. Brooker*,§

Department of Biochemistry, Molecular Biology, and Biophysics, College of Biological Sciences, and Biological Process Technology Institute, University of Minnesota, St. Paul, Minnesota 55108

Received May 15, 1998; Revised Manuscript Received July 29, 1998

ABSTRACT: The lactose permease, encoded by the *lacY* gene of *Escherichia coli*, is an integral membrane protein that functions as a proton and lactose symporter. In this study, we have characterized a novel monodisperse, purified preparation of lactose permease, as well as functionally reconstituted lactose permease, using spectroscopic techniques. The purification of monodisperse lactose permease has been aided by the development of a *lacY* gene product containing an amino-terminal six histidine affinity tag. In the novel purification method described here, lactose permease is purified from *β*-dodecyl maltoside-solubilized membrane vesicles using three sequential column steps: hydroxyapatite, nickel−nitriloacetic acid (Ni−NTA) affinity, and cation-exchange chromatography. The hydroxyapatite step was shown to be essential in reducing aggregation of the final purified protein. Amino acid composition analysis and sodium dodecyl sulfate−polyacrylamide gel electrophoresis (SDS−PAGE) analysis support the conclusion that the protein has been purified to greater than 90% homogeneity. The protein has been successfully reconstituted and has been shown to be active for lactose transport. Fourier transform infrared (FT-IR) spectroscopy has been performed on monodisperse lactose permease and on proteoliposomes containing functional lactose permease. FT-IR spectroscopy supports the conclusion that the monodisperse lactose permease preparation is 80% α-helical and stably folded at 20 °C; thermal denaturation is first detected at 70 °C. Because the purified protein is also readily susceptible to ^{2}H exchange, these results suggest that the protein is conformationally flexible and that ^{2}H exchange is facilitated as the result of conformational fluctuations from the folded state.

The uptake of solutes, including necessary metabolites, is a crucial requirement for the proliferation of cells. To date, a wide variety of proteins that play a role in the process of solute uptake have been characterized (for review see ref *1*). Many of these proteins belong to the major facilitator superfamily (MFS)[1] (*2*−*4*). The lactose permease of *Escherichia coli* belongs to the MFS and has been studied as a model for transport phenomena (*5*). The lactose permease functions as a *β*-galactoside and proton symporter. This protein translocates lactose and protons across the cell membrane with a 1:1 stoichiometry (*6*). The protein catalyzes the accumulation of lactose against a concentration gradient using the free energy contained within a proton electrochemical gradient as the driving force (*7*).

The *lacY* gene encodes the lactose permease. The gene has been cloned into recombinant plasmids and sequenced (*8*). The *lacY* gene product consists of 417 amino acids and has a predicted molecular mass of 46.5 kDa (*8, 9*). On the basis of hydropathy analysis, the protein is predicted to contain 12 transmembrane spanning α-helical domains (*10*). This prediction has been supported by circular dichroism, limited proteolysis, chemical modification, and analysis of a series of lactose permease−alkaline phosphatase fusion proteins (*10*−*13*). Antibody binding studies show that the amino- and carboxyl-terminal segments are located in the cytoplasm (*14*−*16*). An extensive set of lactose permease mutants has been generated and characterized (*17*−*24*). Mutations at certain key amino acids are known to perturb the function (for review, see ref *24*).

† This work was supported from Grant GM53259 from the National Institutes of Health. J.S.P. was partially supported by training grant GM08347-09 from the National Institutes of Health.

* To whom correspondence should be addressed. R.J.B.: Bioprocess Technology Institute, 240 Gortner Laboratory, 1479 Gortner Ave., St. Paul, MN 55108; email robert-b@biosci.cbs.umn.edu. B.A.B.: Department of Biochemistry, 140 Gortner Laboratory, 1479 Gortner Ave., St. Paul, MN 55108; email barry@biosci.cbs.umn.edu.

‡ Department of Biochemistry, Molecular Biology, and Biophysics.

§ Biological Process Technology Institute.

[1] Abbreviations: BCIP/NBT, 5-bromo-4-chloro-3-indolyl phosphate/nitroblue tetrazolium; BSA, bovine serum albumin; CCCP, carbonyl cyanide *m*-chlorophenyl hydrazone; cmc, critical micelle concentration; DM, *β*-dodecyl maltoside; EDTA, ethylenediaminetetraacetic acid; EPR, electron paramagnetic resonance spectroscopy; FT-IR, Fourier transform infrared spectroscopy; HEPES, *N*-(2-hydroxyethyl)piperazine-*N*′-2-ethanesulfonic acid; IPTG, isopropyl *β*-D-thiogalactoside; MES, 2-(*N*-morpholino)ethanesulfonic acid; MFS, multiple facilitator superfamily; MWCO, molecular weight cutoff; Ni−NTA, nickel−nitriloacetic acid; PE, phosphatidylethanolamine; PG, phosphatidylglycerol; PMSF, phenylmethane sulfonyl fluoride; RMS, root-mean-square; SDS−PAGE, sodium dodecyl sulfate−polyacrylamide gel electrophoresis; TDG, D-galactopyranosyl *β*-D-thiogalactopyranoside; TES, *N*-tris(hydroxymethyl)methyl-2-aminoethanesulfonic acid; TPCK, *N*-tosyl-L-phenylalanine chloromethyl ketone; YT, yeast tryptone.

10.1021/bi981142x CCC: $15.00
Published on Web 10/16/1998

We have proposed a tertiary structural model for the lactose permease (see ref *25*). This model postulates rotational symmetry between the two conserved halves of the protein. However, there is no atomic-level structure of the protein. More recently, a variety of biophysical techniques have been used to obtain structural information. Spin labels have been engineered within loops and helices of the lactose permease, and EPR studies have been performed to determine distance relationships between spin labels (*26*, *27*). Intermolecular metal binding sites have been designed for EPR study of distance relationships between specific amino acid residues (*28*−*30*). Fluorescence labeling assays have been performed to determine helical arrangement within the membrane (*31*, *32*). These methods have provided valuable information about the secondary and tertiary structure of the protein.

Fourier transform infrared spectroscopy (FT-IR) is another important technique in the analysis of protein structure and structural changes (for review see refs *33* and *34*). This technique can provide information regarding protein secondary structure and ionization of functional groups within a protein and can be used to probe structural changes of a conformationally active protein. In this study, we report a purification method that yields a monodisperse, highly purified preparation of the lactose permease that is primarily in the monomeric form. We report the first, detailed FT-IR-derived structural characterization of the monodisperse, monomeric protein in detergent micelles. FT-IR spectra were also obtained on proteoliposomes containing reconstituted, functional lactose permease.

EXPERIMENTAL PROCEDURES

Materials

E. coli growth medium was obtained from Bio-101 Inc. (Vista, CA). IPTG, ampicillin, PMSF, DNase I (EC 3.1.21.1, type IV), ultrapure glycine, BSA, MES, and lactose were obtained from Sigma (St. Louis, MO). The lactose was recrystallized to remove impurities prior to use (*35*). β-Dodecyl maltoside and sodium cholate were purchased from Anatrace (Maumee, OH). Imidazole was from Boehinger-Mannheim (Indianapolis, IN), Acetone/ether-washed *E. coli* total lipids, PE, and PG were from Avanti Polar Lipids (Alabaster, AL). TES was from Fisher Biotech (Pittsburgh, PA) and ultrapure glycerol was obtained from Gibco-BRL (Gaitherburg, MD). Pepstatin and TPCK were from Calbiochem (La Jolla, CA). Ni−NTA agarose beads were from Qiagen (Valencia, CA), and Bio-Gel HT hydroxyapatite was from Bio-Rad (Hercules, CA). [^{14}C]Lactose (300 μCi/mmol) was purchased from Amersham (Arlington Heights, IL). Dialysis tubing (6−8 and 12−14 kDa MWCO) was purchased from Spectrum (Houston, TX) and was treated to remove proteases by boiling three times in 5 mM EDTA. Deuterium oxide (^{2}H, 99.9%) and sodium deuterioxide (^{2}H, 99.5%) were purchased from Cambridge Isotope Laboratories (Andover, MD). All other materials were analytical grade and were obtained from commercial sources.

Methods

Bacterial Strains and Cell Growth. By use of the QIA express system (Qiagen, Valencia, CA), a *lacY* fusion protein was engineered to produce a lactose permease containing a 6× histidine affinity tag at the amino terminus. To make the fusion protein, a *Bam*HI site was introduced nine base pairs upstream of the start codon in the *lacY* gene via site-directed mutagenesis. The *Bam*HI fragment, containing the entire *lacY* coding sequence, was then cloned into a plasmid, pQE30 (obtained from Qiagen express system), thus adding 13 amino acid residues (including the six histidines) to the amino terminus of the lactose permease (Figure 1). The methionine residue at position 14 is the normal start methionine present in the wild-type permease. The upstream promoter in pQE30 is highly active, so this construct leads to effective IPTG-inducible expression of the fusion protein. Also, the promoter in pQE30 is tightly controlled by two tandem *lac* operator sites, so that uninduced levels of the fusion protein are very low. The plasmid encoding the *lacY* fusion protein was designated pQE30−*lacY*.

*M-R-G-S-**H-H-H-H-H-H**-G-S-I-M-Y-Y-L-K-N-T-N-*

F-W-First Transmembrane Domain---

FIGURE 1: Amino acid sequence at the NH_2 end of the 6-His−lactose permease fusion protein.

pQE30−*lacY* was transformed into T184 (*36*), a *lacY*-negative strain of *E. coli*. The cells containing the *lacY* fusion protein were stored at −80 °C in glycerol cultures. Single colonies isolated on YT-amp plates, containing 10 g of tryptone, 5 g of yeast extract, 5 g of NaCl, 10 g of agar, and 0.1 mg/mL ampicillin per liter, were used to inoculate YT-amp 50 mL starter cultures, which were then used to inoculate 1−5 L cultures. For larger cultures (5−20 L), 1% glycerol was added to supplement the growth medium. Cells, induced with 2 mM IPTG or 30 mM lactose at late log phase, were grown for 1−2 h and were harvested with centrifugation at 10000*g* for 10 min. Cells were frozen at −80 °C after harvesting.

Determination of Protein Concentration. The amount of protein obtained from various steps of the purification protocol was determined by the Bradford method (*37*). For measurements on protein−detergent micelles, a protein standard curve was generated from BSA and DM in the appropriate buffer. For measurements on reconstituted protein samples, phospholipids were also included in the standard curve. Protein concentration was determined by monitoring the absorption at 595 nm through the use of a Hitachi U-3000 spectrophotometer and correction with a buffer blank.

Isolation of Membrane Vesicles. For isolation of membrane vesicles, cells were resuspended in French press buffer (50 mM TES−NaOH, pH 8.0, 100 mM NaCl, and 5 mM β-mercaptoethanol) to a final cell concentration of 0.2 g of cell wet weight/mL. The following protease inhibitors were added: TPCK (0.1 mg/mL), pepstatin (0.7 μg/mL), and PMSF (25 μg/mL). A stock solution of PMSF was made up in 95% ethanol and stored at −20 °C. DNase I (10 μg/mL) was added to digest plasmid DNA. Cells were broken at 4 °C by a French press at 20000 psi. Cell debris was pelleted with three low-speed spins of 20000*g* for 10 min. The membrane vesicles were collected by ultracentrifugation at 180000*g* for 45 min, were washed once with French press buffer, and were centrifuged a second time at 180000*g* for 45 min. The final membrane vesicle pellet was resuspended

in hydroxyapatite start buffer (HAS buffer: 50 mM TES−NaOH, pH 8.0, 100 mM NaCl, 20% glycerol, 5 mM β-mercaptoethanol, and 1 mM lactose). The protein was diluted to a concentration of approximately 10 mg/mL and was stored at −80 °C prior to solubilization.

Solubilization of Membrane Vesicles. Membranes were diluted with HAS buffer to achieve a final protein concentration of 1.0 mg/mL after solubilization. Solubilization was carried out in HAS buffer on ice with continuous mixing. A stock solution of 5% DM was added dropwise to the membranes to a final concentration of 1%. The membranes were solubilized on ice with shaking for 1 h after the addition of DM. Nonsolubilized material was removed by ultracentrifugation at 180000*g* for 45 min at 4 °C. The solubilized material in the supernatant was loaded directly onto a hydroxyapatite column following the centrifugation step.

Column Buffers and Conditions. The hydroxyapatite column was equilibrated with two column volumes of HAS buffer, followed by two column volumes of hydroxyapatite elution buffer (HAE buffer: 50 mM TES−NaOH, pH 8.0, 1 M NaCl, 350 mM $K_2H_2PO_4$, 20% glycerol, 5 mM β-mercaptoethanol, and 1 mM lactose). Finally, the column was equilibrated with two column volumes of HAS buffer. Two milliliters of bead slurry was employed for every 5 mg of protein. The flow rate was maintained at less than 1.0 mL/min. Approximately 75−85% of the solubilized protein was found to bind to the column. The column eluate was monitored with a Pharmacia UV monitor at 280 nm with a 0.2 mm path length flow cell. After protein loading, the column was washed with HAS buffer containing 0.05% DM until the A_{280} stabilized near zero absorbance. The bound protein was eluted through the application of HAE buffer containing 0.05% DM. The eluted protein was collected and pooled for Ni−NTA batch binding.

Ni−NTA agarose affinity beads were equilibrated with two column volumes of Ni−NTA start buffer (NiS buffer: 50 mM TES−NaOH, pH 8.0, 100 mM NaCl, 15 mM imidazole, 20% glycerol, 5 mM β-mercaptoethanol, 1 mM lactose, and 0.05% DM). The beads were then equilibrated with two column volumes of Ni−NTA elution buffer (NiE buffer: 50 mM TES−NaOH, pH 8.0, 100 mM NaCl, 250 mM imidazole, 20% glycerol, 5 mM β-mercaptoethanol, 1 mM lactose, and 0.05% DM). Finally, the beads were equilibrated with two column volumes of NiS buffer.

Ni−NTA beads were added to the pooled protein mixture from the hydroxyapatite column. The ratio of Ni−NTA agarose beads to protein was 2 mL of bead slurry/10 mg of protein. The protein, which had eluted from the hydroxyapatite column, was incubated with Ni−NTA agarose beads on ice with shaking for 1 h. After batch binding, the beads were poured into a column, which was run at a flow rate of less than 0.25 mL/min. The column was washed with NiS buffer and monitored at 280 nm as previously described. When a stable baseline was reached, the bound protein was eluted by the addition of NiE buffer. A sharp peak of protein elution was observed at approximately 50−75 mM imidazole. To remove imidazole and salts, the eluted protein was pooled and dialyzed in 6−8 kDa MWCO dialysis tubing overnight in dialysis buffer, containing 50 mM TES−NaOH, pH 8.0, 100 mM NaCl, 20% glycerol, and 5 mM β-mercaptoethanol. A buffer volume 100 times the sample volume was used (100:1 v/v).

A 1/1 Mono S cation-exchange FPLC column was equilibrated with two column volumes of Mono S elution buffer (MSE buffer: 50 mM TES−NaOH, pH 8.0, 2 M NaCl, 20% glycerol, 5 mM β-mercaptoethanol, 1 mM lactose, and 0.05% DM), followed by 5 column volumes of Mono S start buffer (MSS buffer: 50 mM TES−NaOH, pH 8.0, 100 mM NaCl, 20% glycerol, 5 mM β-mercaptoethanol, 1 mM lactose, and 0.05% DM) at a flow rate of 0.5 mL/min. The sample was loaded with a 1.5 mL loop or a 50 mL superloop (Pharmacia, Uppsala Sweden). After the protein was loaded, the column was washed with MSS buffer. The lactose permease fraction did not bind to the column and was collected in the flow-through fractions and pooled. The lactose permease fraction was stored at −20 °C.

SDS−PAGE, Silver Staining, and Western Analysis. The purity of the lactose permease was determined by SDS−PAGE containing 12% acrylamide:0.3% bisacrylamide (*38*). Protein samples were solubilized in buffer containing 2% SDS, 10 mM β-mercaptoethanol, 20% glycerol, and bromophenol blue for 30 min at room temperature. Gels were silver-stained by an ammonia-based method (*39*). For Western blot analysis, protein samples were transferred to nitrocellulose with a Semi-Phor semidry electroblotting apparatus (Hoefer, San Francisco, CA) for 30 min at 100 mA. The transferred proteins were probed with an antibody that recognizes the carboxyl terminus of the lactose permease (kindly provided by T. H. Wilson, Harvard University). The primary antibody was detected with a secondary goat anti-rabbit IgG−alkaline phosphatase conjugate antibody (Sigma Immuno Chemicals, St. Louis, MO). Blots were visualized by developing the alkaline phosphatase with Sigma Fast BCIP/NBT tablets (Sigma, St. Louis, MO) (*40*).

Amino Acid Composition Analysis and N-Terminal Protein Sequencing. For amino acid composition analysis, purified protein was subjected to a modified hydrolysis method (*41*). The protein was bound to a nitrocellulose support and the nitrocellulose was washed to remove glycerol, which interferes with amino acid composition analysis. Hydrolyzed samples were run on a Beckman 6300 amino acid analyzer with a 50 μL injection loop and a 12 cm sodium hydrolysate ion exchange column using postcolumn derivitization with ninhydrin. Data were acquired and analyzed on a Beckman System Gold Data system using software version 8.1 (Beckman, Fullerton, CA). Area under peaks of a set of amino acid standards was used to determine concentrations of individual amino acid residues in the protein sample. Experimentally determined amino acid composition was compared to the predicted composition of lactose permease including the additional 13 amino acids comprising the affinity tail.

For N-terminal amino acid sequencing, samples were sequenced on an Applied Biosystems Incorporated 470 gas-phase peptide sequencer with on-line phenylthiohydantoin (PTH) amino acid analysis. Samples were run with the normal sequencing cycles and were backed with a precycled polybrene-coated filter. Data were acquired and analyzed on a Beckman System Gold Data system.

Reconstitution of Lactose Permease into Liposomes. E. coli acetone/ether-washed total lipids were solubilized with 2% sodium cholate in 75 mM HEPES−KOH (pH 7.4). To aid solubilization, the solution was sonicated for 1 min (or until clear) with a point sonicator with a microtip (Biosonik

sonicator, Bronwill Scientific, Rochester, NY). Lipids were maintained under argon to avoid oxidation. Nonsolubilized lipids and titanium particles were removed by ultracentrifugation at 180000*g* for 30 min at 4 °C. Purified lactose permease, in DM micelles, was incubated with 2% sodium cholate for 1 h prior to reconstitution. Lactose permease was then mixed with solubilized lipids at a 1:20 or 1:50 weight ratio and placed into 12−14 kDa MWCO dialysis tubing. The protein and lipid mixture was first dialyzed in buffer containing 75 mM HEPES−KOH, pH 7.4, 14 mM KCl, and 0.1% cholate for 6 h. A buffer volume 100 times the sample volume was employed (100:1 v/v). The second dialysis was in 75 mM HEPES−KOH, pH 7.4, and 14 mM KCl for 6 h (100:1 v/v). The third dialysis was in 50 mM HEPES−KOH, pH 7.4, 25 mM KCl, and 15 mM sucrose or lactose for 12 h (100:1 v/v). The final dialysis was in 10 mM HEPES−KOH, pH 7.4, 45 mM KCl, and 45 mM sucrose or lactose for 12 h (500:1 v/v). Proteoliposomes were collected by ultracentrifugation at 180000*g* for 30 min at 4 °C. Proteoliposomes were resuspended in 50 mM phosphate buffer (pH 6.0) with or without 20 mM lactose (loaded or unloaded vesicles) and stored at 4 °C. Liposomes derived from total *E. coli* lipids or from PE:PG (3:1) were prepared by the methods described above, omitting the protein addition step.

Sugar Transport Assay (Counterflow Assay). Counterflow assays were performed on lactose-loaded or unloaded proteoliposomes made on the same day or after storage at 4° C. For each assay, 15 μL (0.5 mg/mL) of proteoliposome vesicles was resuspended in 525 μL of 100 mM phosphate buffer, pH 6.0, containing 2 mM $MgSO_4$, 1.0 μCi of [^{14}C]-lactose, and 1 mM lactose. For assays with TDG (50 mM fresh stock made in phosphate buffer) or CCCP (10 mM fresh stock prepared in ethanol), a 1 mM or 10 μM final concentration was added to the assay buffer, respectively. Assays were performed at 25° C. A 100 μL sample of the reaction volume was collected at various time points and was aliquoted onto a 0.45 μm nitrocellulose filter disk. The disk was washed several times with 100 mM phosphate buffer, pH 6.0. The filter disks were placed into 2 mL of scintillation fluid and the amount of [^{14}C]lactose exchange into the vesicles was determined by scintillation counting. Protein concentrations were estimated by Bradford assays (see above).

Deuterium Exchange. The lactose permease in detergent micelles was ^{2}H-exchanged by repeated dilution and concentration in a ^2H_2O buffer with Centricon 30 concentrating units (Amicon, Beverly, MA). This exchange procedure was performed at 6 °C and typically required 5−6 h. Once exchanged, samples were aliquoted and frozen at −80 °C. Buffers containing either 5 mM MES−NaO^{2}H and 0.03% DM, p^{2}H 5.5, or 5 mM TES−NaO^{2}H and 0.03% DM, p^{2}H 8.0, were used; the p^{2}H is reported as the uncorrected meter reading (*42*).

Proteoliposomes were deuterium-exchanged by a series of ultracentrifugation steps in ^{2}H buffers. Proteoliposomes were pelleted at 180000*g* for 45 min. The pellet was resuspended in ^{2}H buffer and incubated for 4−6 h. Proteoliposomes were repelleted as above. The final pellet was resuspended in a small volume of ^{2}H buffer and stored at 4 °C.

UV−Vis Spectroscopy. Spectra of lactose permease in detergent micelles were acquired through the use of a Hitachi U-3000 spectrophotometer. Spectral conditions were as follows: 60 nm/min scan rate and 2.0 nm slit width. The spectra of lactose permease were buffer-subtracted.

FT-IR Spectroscopy. Spectra of lactose permease in detergent micelles and proteoliposomes, containing lactose permease, were acquired through the use of a Magna II Nicolet spectrometer equipped with a liquid nitrogen-cooled MCT-A detector and a KBr beam splitter. The mirror velocity was 2.53 cm s^{-1}, the spectral resolution was 2 cm^{-1}, and 2000 mirror scans were coadded for each double-sided interferogram. A Happ−Genzel apodization function and one additional level of zero-filling were used. Peak positions are known to ±1 cm^{-1}. The monodisperse protein samples had a concentration of 15−30 mg/mL and were suspended in ^2H_2O buffers. Six microliters of sample was placed between two 19 mm CaF_2 windows (Harrick Scientific, Ossining, NY) with a 6 μm spacer. Proteoliposomes, liposomes derived from total *E. coli* lipids, or liposomes derived from PE:PG (3:1 ratio) were prepared for FT-IR spectroscopy by drying 20−40 μL of sample onto a CaF_2-window under a constant stream of nitrogen. Protein reconstitution was performed as described above at a 1:15 protein-to-lipid ratio. Proteoliposomes contained 1−3 mg/mL protein as determined by Bradford assays.

For FT-IR experiments, the sample holders and temperature control units have been previously described (*43*). For studies of monodisperse lactose permease, a spectrum of the appropriate buffer alone was recorded at both 20 and 90 °C. This spectrum was subtracted from the protein spectrum on a noninteractive 1:1 basis; these data were recorded on the same day. For the temperature study, spectra of the same protein sample were taken sequentially at 20, 30, 50, 70, 90, and 20 °C. Fourier deconvolution, second-derivative analysis, and nonlinear regression analysis were performed with Nicolet Omnic and Grams software, as described (*43*). Fourier deconvolution requires the choice of line width parameter, resolution enhancement parameter (K), and apodization function. The enhancement parameter ($K = 2$) was chosen in accord with signal-to-noise criteria previously described (*44*). The line width parameter (40 cm^{-1}) was chosen on the basis of spectra previously derived (*45*). Our somewhat conservative choices for line width parameter and enhancement parameter resulted in the derivation of the minimum number of spectral components necessary to fit the data. A modified Happ−Genzel function was employed for apodization. All spectra were analyzed under the same conditions. Second-derivative analysis employed a Savitsky−Golay smoothing procedure, as previously described (*46*).

RESULTS

Purification of the Lactose Permease. A method for the purification of lactose permease from solubilized membrane vesicles has been developed. The primary purification step involves the use of an affinity tag engineered onto the amino-terminal end of lactose permease. This six-histidine tag causes the protein to bind to a nickel chelate affinity support. The use of nickel chelate affinity chromatography has been described for the successful purification of a number of

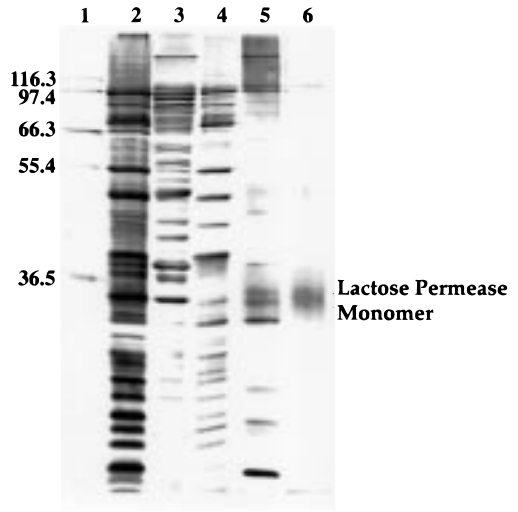

FIGURE 2: SDS−PAGE analysis of samples from various stages of the lactose permease solubilization/purification procedure. Protein samples were solubilized in buffer containing SDS and were incubated at room temperature for 30 min. Proteins were resolved on 12% acrylamide gels and were visualized by silver staining. Lane 1, molecular mass markers (kilodaltons); lane 2, membrane vesicles (1 μg); lane 3, DM-solubilized membrane vesicles (1 μg); lane 4, samples obtained after hydroxyapatite chromatography (2 μg); lane 5, samples obtained after Ni−NTA chromatography (5 μg), and lane 6, samples obtained after cation-exchange chromatography (10 μg).

soluble and membrane-bound proteins (*47*−*52*). Our method for obtaining monodisperse lactose permease also includes an initial hydroxyapatite column and a final cation-exchange column.

In Figure 2, we present a silver-stained gel, derived from SDS−PAGE, of protein fractions obtained from each step of the purification. Lanes 2 and 3 show the electrophoretic pattern obtained from membrane vesicles and solubilized vesicles, respectively, which contain a complex mixture of proteins. Lanes 4, 5, and 6 show the pattern obtained after hydroxyapatite, Ni−NTA, and cation-exchange chromatography, respectively. The inclusion of an hydroxyapatite column does not afford significant purification on a protein basis (Figure 2, lane 4) but does serve to reduce aggregation (shown below). Since the hydroxyapatite column employed buffer conditions compatible with the nickel affinity step, the eluted fractions from the hydroxyapatite column were bound directly to the Ni−NTA agarose beads. This procedure eliminated time-consuming buffer exchanges by dialysis or desalting procedures. The samples obtained after the Ni−NTA chromatography show significant enrichment for lactose permease (Figure 2, lane 5).

To further reduce protein contamination, a third chromatography step involving a Mono S cation-exchange column was employed (Figure 2, lane 6). This column binds contaminating proteins, whereas the lactose permease does not bind and is eluted in the flowthrough volume. After completion of the purification, one major silver-stained band is observed (Figure 2, lane 6). This protein is identified as the lactose permease by Western blot analysis (Figure 3, lane 3). The apparent molecular mass of the lactose permease monomer band is 30.3 kDa. An anomalously low molecular mass is common among membrane proteins analyzed by SDS−PAGE and has been previously observed for the lactose permease (*53*). Table 1 summarizes the protein yields

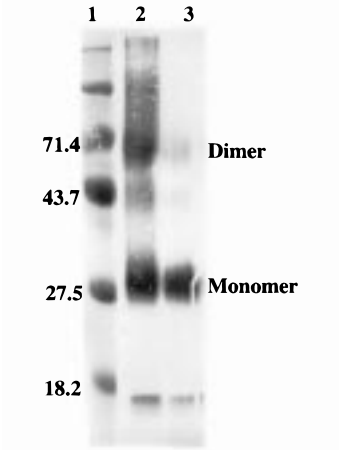

FIGURE 3: Western blot analysis of lactose permease samples showing the effects of the hydroxyapatite column step on protein aggregation. Lane 1, prestained molecular mass markers (kilodaltons); lane 2, purified lactose permease prepared without the use of hydroxyapatite chromatography (10 μg); and lane 3, purified lactose permease sample prepared with the inclusion of hydroxyapatite chromatography (10 μg). Both samples were subjected to Ni−NTA and cation-exchange chromatography.

Table 1: Yields of Protein during the Purification of the Lactose Permease

purification step	total protein (mg)
DM-solubilized membranes	300
hydroxyapatite column	240
nickel affinity column	7.5
cation-exchange column	4.5

at the various steps in the purification procedure; the overall yield is 1.5% on a total protein basis.

Our initial attempts at purification of lactose permease showed that the nickel affinity method would not be sufficient for optimal purification. Moreover, when purifying proteins from bacterial sources, aggregation can be a significant problem (*54*). Such aggregation makes it difficult to remove protein contaminants, interferes with biophysical measurements and crystallization, and can interfere with the reconstitution of the protein into liposomes.

Previously, it was determined that the inclusion of hydroxyapatite chromatography significantly reduced aggregation in preparations of a bacterial cytochrome *c* oxidase (*54*). In Figure 3, we show data demonstrating that the inclusion of an initial hydroxyapatite column treatment in our lactose permease purification (Figure 3, lane 3) significantly reduced the amount of protein aggregation in the final product when compared to an identical purification procedure that did not include the hydroxyapatite column (Figure 3, lane 2). Comparison of lanes 2 and 3 shows that use of the hydroxyapatite chromatography results in a decrease in the amount of dimerized and trimerized lactose permease.

The degree of protein aggregation in samples of lactose permease, purified without hydroxyapatite chromatography, was also determined by measuring the amount of sedimenting protein. The sample was subjected to a short (45 min), high-speed (180000*g*) ultracentrifugation. Protein concentrations before and after this step were determined by use of a Bradford assay and by measuring the protein absorbance at 280 nm. The results showed that sedimentation occurred for a substantial amount of the purified protein (51% ± 9%).

Table 2: Amino Acid Composition of Purified 6× His-Tagged Lactose Permease

amino acid	determined	expected	amino acid	determined	expected
Asx	28	22	Met	16	15
Thr	21	19	Ile	30	34
Ser	26	31	Leu	48	54
Glx	30	22	Tyr	11	14
Pro	13	12	Phe	37	56
Gly	36	38	His	12	10
Ala	34	35	Lys	14	12
Cys	7	8	Arg	14	13
Val	31	29	Trp	ND[a]	6

[a] Not determined.

This same procedure performed on hydroxyapatite-treated purified lactose permease resulted in only 6% ± 3% loss of protein due to sedimentation. These results indicate that much of the lactose permease, purified without hydroxyapatite chromatography, is in an aggregated state.

Amino Acid Composition and N-Terminal Sequencing of the Purified Lactose Permease. Table 2 gives the results of amino acid composition analysis of the purified lactose permease sample. Comparison of the number of moles of amino acids, experimentally derived, with the expected values shows that the lactose permease is ~93% homogeneous. Glycine, alanine, valine, leucine, and isoleucine were used in this calculation because these amino acid side chains are stable under acidic hydrolysis (*55*). The somewhat low values for the aromatic amino acids, when compared to the predicted amino acid sequence, are expected in anaerobic hydrolysis (*55*). N-Terminal amino acid sequencing confirms that the purified protein contains the first eight amino acids, which comprise the start of the histidine tag (Figure 1).

Reconstitution of Lactose Permease and Functional Assays. To verify the activity of the purified lactose permease, the protein was reconstituted into artificial lipid vesicles. The necessity for reconstitution makes it difficult to monitor specific activity changes as a function of the various stages of purification. A number of methods exist for reconstitution of membrane proteins (for review see refs *56*−*60* and references therein). These methods rely on lowering the concentration of detergent below the cmc so that the protein is forced to associate with an alternative hydrophobic environment. Formation of proteoliposomes is spontaneous under these conditions.

The technique of reconstitution found to be the most successful in the present application was a modified dialysis method. This method has been described for the successful reconstitution of another membrane protein, cytochrome oxidase, after purification in β-dodecyl maltoside (*54*). DM has been successfully applied to the purification of many membrane proteins in a monodisperse and functional form (*61*−*63*). However, this detergent has a low cmc, making reconstitution of membrane proteins potentially difficult. We have found that the addition of sodium cholate to DM−lactose permease micelles resulted in an eventual, successful reconstitution by dialysis (*54*). The concentration of sodium cholate is 40-fold greater when compared to dodecyl maltoside; sodium cholate has a higher cmc. Four sequential dialysis steps were employed for the slow removal of detergent. The proteoliposomes obtained from this reconstitution method were analyzed by SDS−PAGE and Western blot analysis and were shown to contain lactose permease (data not shown). We did not attempt reconstitution on non-hydroxyapatite-treated lactose permease because we found evidence for significant protein aggregation in these samples (see above and Figure 3).

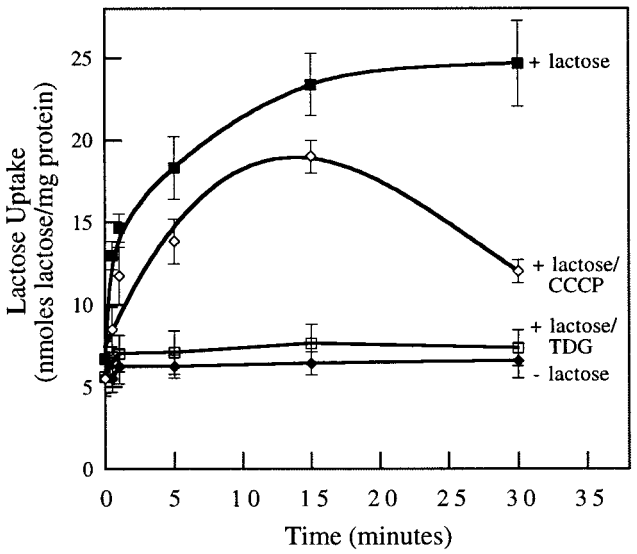

FIGURE 4: Lactose counterflow in proteoliposomes containing reconstituted lactose permease. The assays shown here were performed on proteoliposomes at room temperature in the presence (■) or absence (◆) of lactose, in the presence of lactose and TDG (□), and in the presence of lactose and CCCP (◇) as described under Experimental Procedures. Data presented are the average of 3−6 measurements.

Assays for lactose and proton transport can be performed on reconstituted lactose permease. In Figure 4, we present a counterflow assay, which measures the ability of lactose permease to rapidly exchange lactose from the inside to the outside of the proteoliposome and also measures a slower, unidirectional efflux phase (*64*, *65*). When proteoliposomes were preloaded with lactose, we observed lactose exchange when [^{14}C]lactose was added to the outside of the vesicles (Figure 4, ■). As expected, the control with unloaded proteoliposomes did not accumulate labeled lactose (Figure 4, ◆). Counterflow assays were also performed with the external addition of TDG, which competes for the site of lactose binding. With TDG present we saw no accumulation of labeled lactose, indicating that TDG was successfully competing for the lactose binding site and preventing exchange (Figure 4, □). The initial rate of lactose uptake is difficult to estimate because the earliest possible time point is already near the saturation phase. Due to the time it requires to process the samples, it is not possible to reliably obtain earlier time points through the use of this method. These results demonstrate that we have successfully reconstituted the lactose permease in a functionally active form.

In whole cells or membrane vesicles containing lactose permease, [^{14}C]lactose accumulation rapidly reaches a maximum followed by a slower efflux phase (*21*, *66*). This slow net loss of accumulated [^{14}C]lactose can be attributed to the process of efflux, which involves the symport of protons and lactose down a concentration gradient (inside to outside). In our preloaded proteoliposomes, the efflux process was not observed (Figure 4, ■). One possible explanation of this result might be a decrease in the passive H^+ permeability of the proteoliposomes, when compared to that of cells or

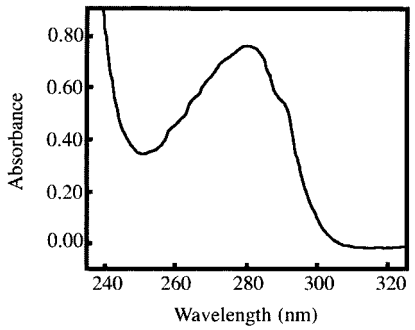

FIGURE 5: UV spectrum of purified, monodisperse lactose permease in MSS buffer showing the 235−325 nm region of the spectrum.

membranes. Normally, whole cells or membrane vesicles show a low level of H^+ permeability, which alleviates the electrochemical gradient caused by the efflux of H^+ with lactose. However, if proteoliposomes containing purified enzyme are impermeant to H^+, the net efflux of H^+ and lactose would yield an H^+ gradient (inside negative) that would quickly inhibit further efflux.

To test this hypothesis, an uncoupler, CCCP, was included in the counterflow assay (*67*). CCCP will dissipate any electrochemical gradient formed in the proteoliposomes that is due to the slower phase of H^+/lactose efflux. In the presence of CCCP, [^{14}C]lactose efflux was observed as a kinetically slower phase (Figure 4, ◇). This result indicates that our inability to detect efflux in the absence of CCCP was due to the formation of an H^+ gradient (interior negative) upon net H^+/lactose efflux. Furthermore, these results suggest that our vesicle preparation is impermeable to the passive flux of H^+ ions.

Spectroscopic Characterization of the Purified Lactose Permease in Detergent Micelles. In Figure 5, we present the UV spectrum of the purified protein. Well-resolved peaks from aromatic amino acids are observed at 280 and 291 nm with smaller contributions at 265 and 269 nm. This spectrum is useful as a verification for successful purification. The protein had no detectable absorption in the visible region of the spectrum, consistent with the absence of bound prosthetic groups (data not shown).

In Figure 6, panels B and C, we present FT-IR spectra of the lactose permease. The protein is in DM micelles and ^{2}H-containing buffers at either p^{2}H 5.5 (Figure 6B) or p^{2}H 8.0 (Figure 6C). There are three possible contributions in the spectral region shown for ^{2}H-exchanged proteins (*68, 69*). The amide I band (approximately 1650 cm^{-1}) is primarily the C═O stretching vibration of the peptide backbone. The amide II band (approximately 1550 cm^{-1}) is a coupled C−N stretch and N−H in-plane deformation mode. These vibrational modes are delocalized and involve simultaneous atomic displacements of the peptide bonds (*68*). In portions of the protein accessible to isotope exchange, replacement of N-^{1}H with N-^{2}H results in a downshift and uncoupling of the C−N and N−^{2}H vibrations (*68*). The amide II band then decreases in amplitude, and new intensity is observed at lower frequencies. In the spectral region shown here, new intensity would be observed at 1450 cm^{-1} upon ^{2}H exchange; this band is called the amide II′ vibrational mode. The amide I′ band shows less dramatic changes upon ^{2}H exchange (*46*).

In ^2H_2O buffers, the lactose permease exhibits an amide I′ vibrational mode with a maximum at 1654 ± 1 cm^{-1}, a

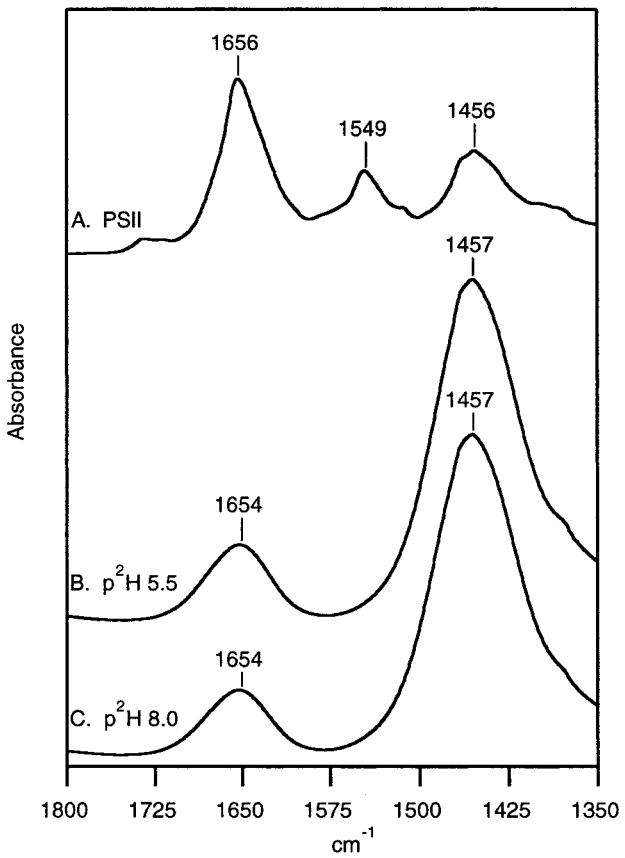

FIGURE 6: FT-IR spectra of ^{2}H-exchanged proteins in β-dodecyl maltoside micelles. Spectra were obtained on lactose permease at p^{2}H 5.5 (B) and p^{2}H 8.0 (C). In trace A, spectra were obtained on photosystem II at p^{2}H 6.5 in DM micelles (*71*).

frequency that is characteristic of α-helical proteins (*46*; and see discussion below), and an amide II′ vibrational mode with a maximum at 1457 ± 1 cm^{-1} (Figure 6B,C). There is no significant intensity in the 1550 cm^{-1} region, either at p^{2}H 5.5 (Figure 6B) or p^{2}H 8.0 (Figure 6C). This is unusual, since α-helical portions of membrane proteins, such as bacteriorhodopsin, have been found to be highly resistant to exchange (*70*). With bacteriorhodopsin, even rigorous exchange protocols failed to exchange 70% of the peptide backbone and gave only a 30% change in the amide II band (*70*). The unexchanged portion was assigned to the transmembrane α-helical portions of the protein (*70*). Such resistance to exchange is also illustrated by Figure 6A, which shows the vibrational spectra of another membrane protein, photosystem II, in DM micelles, after 18 h of ^{2}H exchange. A previous estimate of the percent ^{2}H exchange for this protein was 20% (*71*). By contrast, lactose permease shows complete exchange in 4−6 h in ^2H_2O buffers at either p^{2}H 5.5 or 8.0.

Analysis of the amide I′ line shape of the ^{2}H-exchanged lactose permease was then performed (Figure 7). The amide I′ line shape can be viewed as a superposition of spectral components, each derived from a given type of secondary structural element in the protein (*34, 46, 72, 73*). To resolve these spectral components, second-derivative and Fourier deconvolution analysis can be employed (see, for example, refs *34*, *43*, *46*, and *72*−*76*).

Application of these methods to spectra obtained at either p^{2}H 5.5 (Figure 7A) or p^{2}H 8.0 (Figure 7B) shows that the

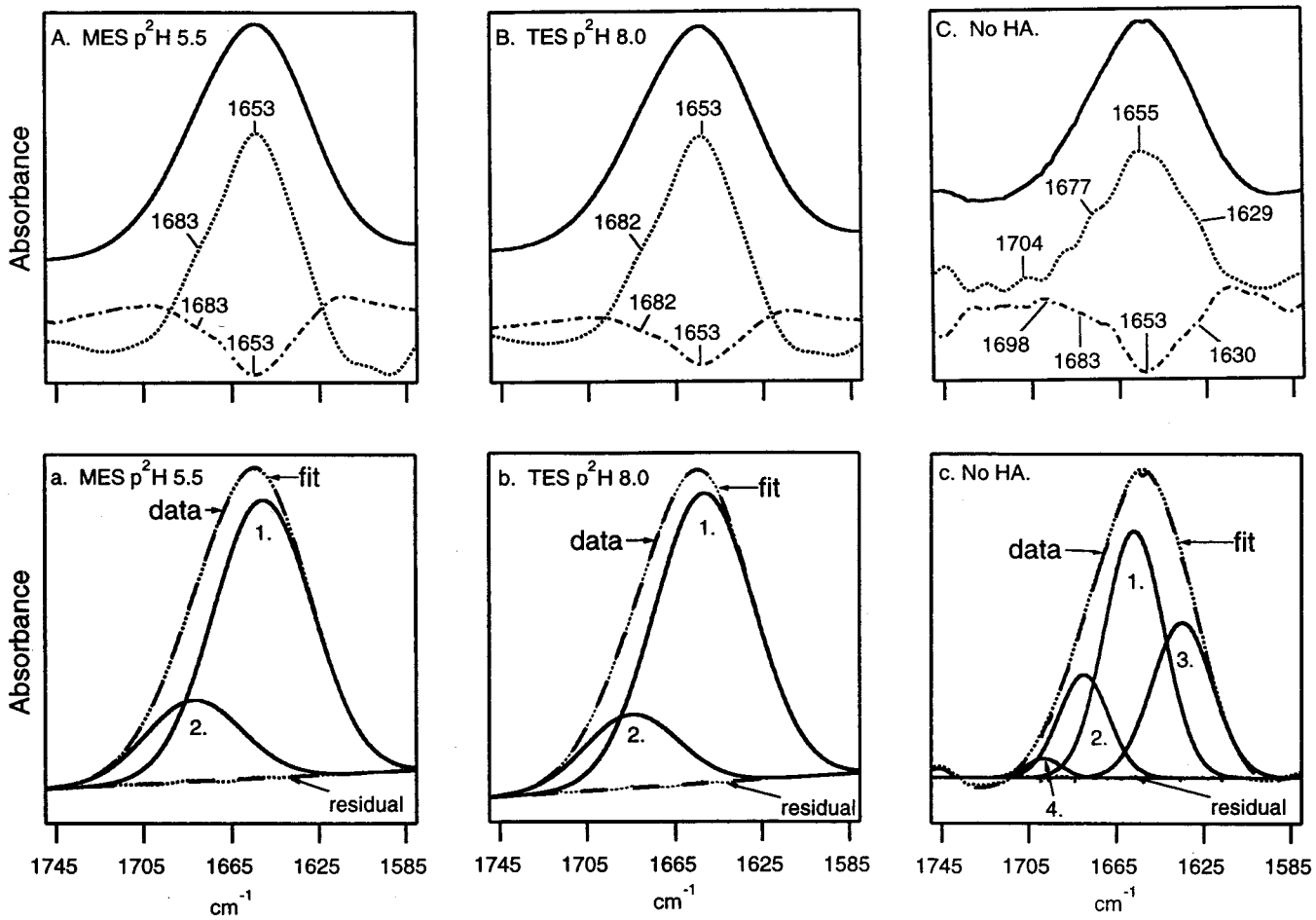

FIGURE 7: Spectral fitting of the amide I′ band of lactose permease. In panels A−C, solid line, spectra were obtained on lactose permease at p^2H 5.5 (A), at p^2H 8.0 (B), and at p^2H 8.0 but without the use of hydroxyapatite chromatography (C). In each panel, the Fourier self-deconvolution and the second derivative of the data are shown as the dotted and dashed lines, respectively. In panels a−c, the results of nonlinear regression analysis of the spectra in panels A−C, respectively, are presented. In panels a−c, the data are shown as the dashed line; the spectrum reconstructed after regression analysis is the dotted line. The spectral components employed in the reconstruction are shown as the numbered Gaussians; the baseline and residual are also presented.

Table 3: Peak Positions and Predicted Secondary Structure of the Lactose Permease As Determined by Analysis of Amide I′ Line Shape

	peak position (cm^{-1})				
	peak 1 [α-helix (%)]	peak 2 [turns (%)]	peak 3 [aggregated/β-strands (%)]	peak 4	peak 5 [denatured (%)]
MES, p^2H 5.5,[a] 20 °C	1651 ± 2 (80 ± 4)	1684 ± 3 (20 ± 4)			
TES, p^2H 8.0,[b] 20 °C	1651 ± 1 (78 ± 3)	1682 ± 2 (22 ± 3)			
TES, p^2H 8.0,[c] 90 °C				1694 ± 2 (6 ± 3)	1649 ± 1 (94 ± 3)
no Hydroxyapatite[d] (TES, p^2H 8.0, 20 °C)	1657 ± 1 (48 ± 3)	1682 ± 2 (17 ± 3)	1636 ± 1 (33 ± 3)	1699 ± 2 (2 ± 1)	

[a] Reduced $\chi^2 = 0.8126$, RMS noise = 0.00012. [b] Reduced $\chi^2 = 0.3703$, RMS noise = 0.00017. [c] Reduced $\chi^2 = 25.775$, RMS noise = 0.00012. [d] Reduced $\chi^2 = 1.7805$, RMS noise = 0.00003.

lactose permease line shape is dominated by one spectral component with a frequency of 1653 ± 1 cm^{-1}. Spectral components with this frequency are typically assigned to α-helix, although turns and loops can make a contribution in this region as well (*34, 46, 72*−*76*). A minor component at 1683 ± 2 cm^{-1} is also observed; this component can be assigned to turns of the protein backbone (*34, 46, 72, 77*−*80*). These frequencies are used as starting points in regression analysis.

Fits of derived spectral components to the amide I′ line shapes, as performed by nonlinear regression, are shown in Figure 7a,b. The fit is satisfactory, as judged by the negligible residual (Figure 7) and by the reduced χ^2 parameter (Table 3). In Table 3, the results of the nonlinear regression analysis are summarized. These data can then be used to predict the secondary structure of the protein. This analysis predicts that 80% ± 4% of lactose permease is α-helical and that 20% ± 4% is involved in turns. There is no significant spectral difference when samples, maintained at p^2H 8.0 and 5.5, are compared (Figure 7a,b).

Figure 7C shows the amide I′ band of lactose permease, purified without the use of hydroxyapatite chromatography. As shown in the Fourier self-deconvolution (FSD) and second-derivative analysis (Figure 7C), additional amide I′ spectral components are now observed. The spectral fit derived through the use of these spectral components is

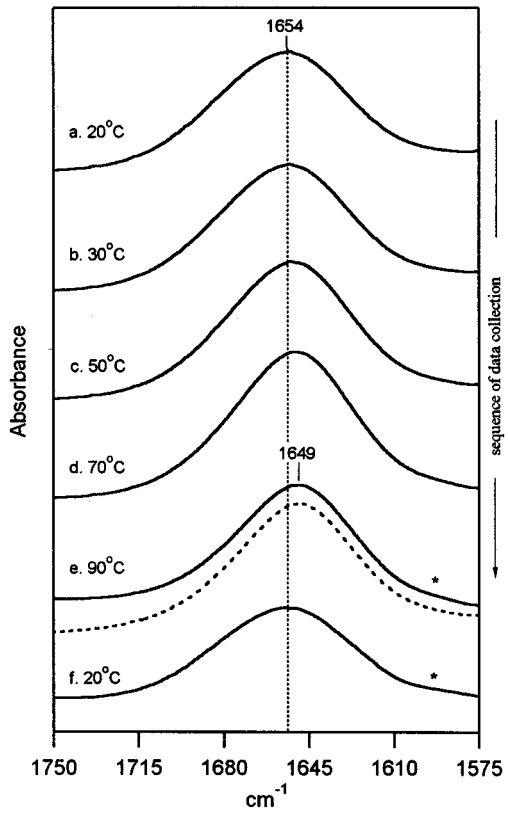

FIGURE 8: FT-IR spectra of ^{2}H-exchanged lactose permease in detergent micelles as a function of increasing temperature. Data were collected as described in Experimental Procedures. Spectra were obtained sequentially on the same lactose permease (p^{2}H 8.0) sample at 20, 30, 50, 70, 90 and 20 °C (traces a−f, respectively). A buffer spectrum taken at 20 °C was subtracted from all the protein samples. The dotted spectrum shows the results of correction, using a buffer spectrum taken at 90 °C (e). This type of correction has no impact on the peak position. Asterisks indicate a new spectral feature at 1595 cm^{-1} (traces e and f).

presented in Figure 7c, and the secondary structural elements predicted from this analysis are presented in Table 3. When hydroxyapatite chromatography is not included in the purification, regression analysis shows that the lactose permease exhibits an additional major spectral component with a frequency of 1636 ± 1 cm^{-1}. A new minor component at 1699 ± 2 cm^{-1} is also observed. These frequencies are typically assigned to β-strands (*46*) but see discussion below.

In Figures 8 and 9, we present a FT-IR experiment, which is designed to define the thermal denaturation of the hydroxyapatite-purified, monomeric protein. Because the amide I line shape is sensitive to structural changes, the FT-IR spectrum can be used to detect denaturation (for example, see refs *76* and *81*−*84*). A downshift of the amide I′ band is expected upon the thermal unfolding of an α-helical protein (*76*, *81*−*84*). In Figure 8, we present data obtained on lactose permease; these data exhibit a 5 cm^{-1} downshift, to 1649 cm^{-1}, as a result of increasing temperature. This is evident in the overlay of the spectra obtained at 20 °C (Figure 9a, dashed line), 90 °C (Figure 9a, solid line), and returned to 20 °C (Figure 9a, dotted line). The downshift of the amide I′ peak is first detected at approximately 70 °C (Figure 8d). The spectral change is mainly reversible upon cooling to 20 °C; a shift of peak position back to 1654 cm^{-1} is observed (Figures 8f and 9a). At 90 °C and after cooling to 20 °C, a new, minor spectral component at 1595 cm^{-1} is detected (Figure 8e,f). We attribute this new spectral feature to thermally induced protein aggregation (*76*, *81*−*84*).

To quantitatively analyze the effect on secondary structure as a result of increasing temperature, curve-fitting was performed on data obtained at 20 °C (Figure 9b) and at 90 °C (Figure 9c). Curve-fitting of the amide I′ line shape at 20 °C (Figure 9b) gives two main spectral components at 1651 and at 1682 cm^{-1}; these components are assigned to α-helix and to turns. Curve-fitting of the amide I′ line shape at 90 °C (Figure 9c) provides evidence for a significant change in secondary structure. The major spectral component is downshifted to 1649 cm^{-1}; this frequency is assigned to random secondary structural elements. Also, the peak previously assigned to turns at 1682 cm^{-1} is no longer observed at 90 °C; a small contribution at 1694 cm^{-1} is obtained. These data are summarized in Table 3; the results are consistent with a change in >90% of the protein's secondary structure upon increasing the temperature to 90° C. These spectra are evidence for a reversible thermal denaturation of the protein at temperatures above approximately 50 °C. These data also indicate that the monomeric protein in detergent micelles is in a stable folded form at 20 °C and is well below its denaturation temperature.

Figure 10, panels a and c show the FT-IR spectra obtained on partially dehydrated proteoliposomes containing reconstituted, functional lactose permease. Spectra were obtained on proteoliposomes in 5 mM TES, pH 8.0 (Figure 10a), and in 5 mM TES, p^{2}H 8.0 (Figure 10c). Deuterium exchange occurred over 4−6 h. As controls, spectra were obtained on liposomes, lacking the permease, under the same conditions (Figure 10b,d). Deuterium exchange of proteoliposomes is observed to downshift the amide I frequency (1655 cm^{-1}) to 1650 cm^{-1} and to downshift the amide II frequency (1544 cm^{-1}) (compare Figure 10, traces a and c). Spectral contributions, attributable to the lipids, at 1739 cm^{-1} (lipid C═O stretching vibrational mode) and 1467 cm^{-1} (methylene scissoring vibrational mode) were not effected by deuterium exchange (compare Figure 10, traces b and d). A spectral feature, centered at 1645 cm^{-1}, is observed in both ^1H_2O and ^2H_2O liposome samples (Figure 10b,d). This lipid-attributable spectral feature is also observed in the proteoliposome spectra. However, the observation of a significant change in the overall shape and frequency of this band is a clear indication that protein is present. Liposomes composed of purified PE and PG (3:1 ratio) were also analyzed, and a similar spectral component, overlapping the amide I region, was observed (data not shown). Efforts to subtract the liposome spectrum from the proteolipsome data were not successful, consistent with an effect of protein reconstitution on the lipid vibrational spectrum.

DISCUSSION

Here, we describe a detailed biochemical and biophysical characterization of a monodisperse, monomeric lactose permease preparation. The method of purification is novel and gives a highly pure product, which is amenable to various methods of characterization. The purification procedure involves three sequential chromatography steps. A hydroxyapatite chromatography step has been shown to be necessary to reduce the amount of aggregated protein (Figure

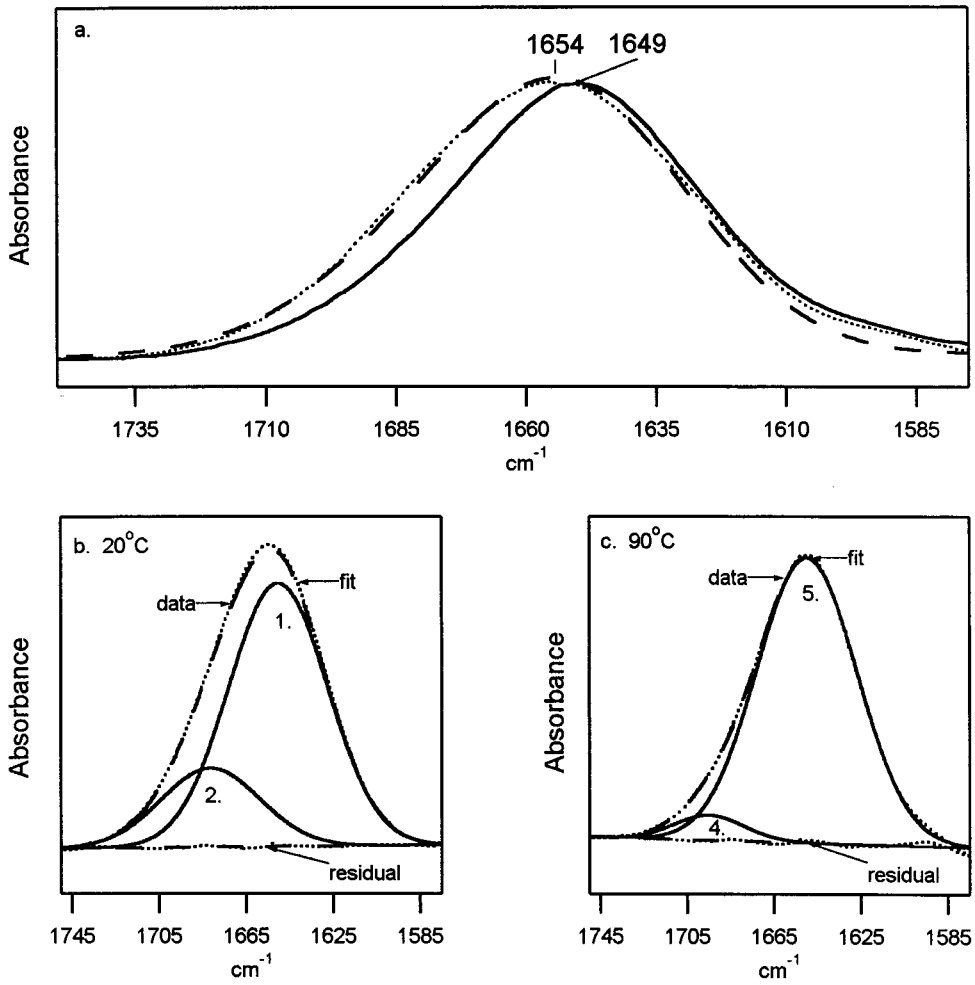

FIGURE 9: FT-IR spectra of ^{2}H-exchanged lactose permease in detergent micelles at 20 and 90 °C and after return to 20 °C (repeated from Figure 8, traces a, e, and f). In panel a, the amide I′ band obtained at 20 °C (dashed line) is superimposed on the amide I′ band obtained at 90 °C (solid line), as well as the amide I′ band obtained after cooling to 20 °C (dotted line). Spectral curve fitting of the amide I′ band obtained at 20 and 90 °C is shown in panels b and c, respectively.

3). Likewise, this step also reduces aggregation in the bacterial membrane protein cytochrome *c* oxidase. Therefore, it may be of general value in the purification of many membrane proteins (*54*). In our purification procedure, a nickel affinity chromatography step affords the bulk of permease purification and enrichment. A final cation-exchange chromatography step was found to remove remaining protein contamination.

We have successfully reconstituted the purified lactose permease using a modified dialysis procedure. The reconstituted proteoliposomes were capable of lactose exchange, which was competitively inhibited by TDG, indicating that the preparation was functionally active. The proteoliposomes formed were impermeant to slow proton leakage as shown by the effects observed upon addition of the proton uncoupler CCCP. Taken together, counterflow assays demonstrate that the purified lactose permease is functionally active.

The purified lactose permease in detergent micelles and proteoliposomes containing functional lactose permease were shown to be suitable for spectroscopic characterization. FT-IR spectroscopy predicts a highly α-helical structure for the monomeric protein in micelles; there is no detectable evidence for intermolecular hydrogen bonding or β-sheet structure (*34, 46, 72*−*81*). A denaturation study shows that the first evidence of protein denaturation is obtained at approximately 70 °C; the spectral change observed is consistent with a conversion of a predominantly α-helical protein to random coil (*34, 46, 72*−*81*). This thermal denaturation is shown to be largely reversible. The cooled, renatured protein shows a small additional spectral component at 1595 cm^{-1}, which we attribute to a small amount of heat-induced aggregation (*81*).

The conclusion that the purified permease in detergent micelles is 80% α-helix is predicted by many previous studies of the lactose permease (*10*−*13*) and is supported by previous circular dichroism and Raman measurements on detergent-solubilized and membrane-associated lactose permease (*10, 85*). However, our results with monodispersed lactose permease are in contrast with those of ref *86*, who attributed infrared spectral components at 1633 cm^{-1} to β-sheet structure. In this study (*86*), lactose permease had not been purified through the use of hydroxyapatite chromatography and had been reconstituted into proteoliposomes by dilution from DM. In monodisperse preparations, we observe additional spectral components, with frequencies in this same spectral region (1636 cm^{-1}), only in aggregated lactose permease samples.

Spectral components at 1636 cm^{-1} are substantially higher in frequency than those attributed to thermally aggregated protein samples (*81*−*84*). For example, our thermal dena-

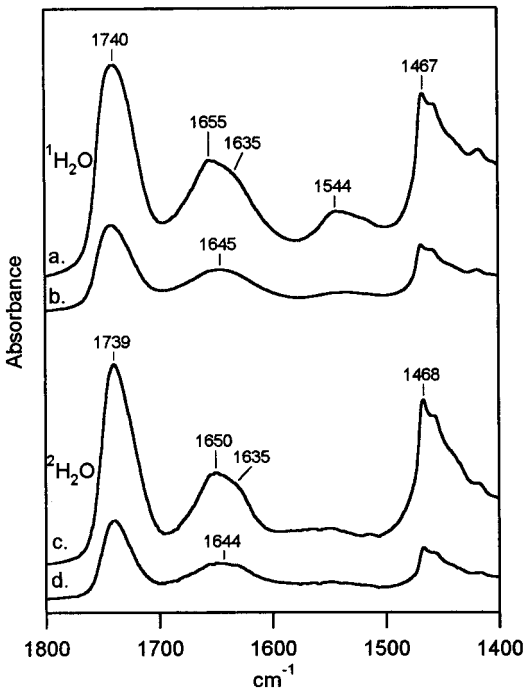

FIGURE 10: FT-IR spectra of proteoliposomes containing lactose permease and liposomes in ^1H_2O or ^2H_2O buffers. Samples were prepared and data were collected as described in Experimental Procedures. Spectra were obtained on proteoliposomes (1:15 protein-to-lipid ratio) and liposomes in 5 mM TES, pH 8.0 (traces a and b, respectively) and on proteoliposomes (1:15 protein-to-lipid ratio) and liposomes exchanged into 5 mM TES, p^{2}H 8.0 (traces c and d, respectively).

turation study shows that heat-induced aggregation results in a new spectral component at 1595 cm^{-1}. Therefore, the origin of these low-frequency amide I′ components in dimeric and trimeric lactose permease is of interest. The observed downshift in frequency from 1657 to 1636 cm^{-1} is generally consistent with an increase in the number or strength of hydrogen bonds. Spectral components in the 1636 cm^{-1} region are usually assigned to β-strands (*34, 46, 72, 77*−*80*). Higher frequency components of lower intensity are also assigned to β-strands (*34, 78, 80*); this may be the origin of the new 1699 cm^{-1} spectral component (Figure 7c), although this frequency is somewhat higher than bands usually assigned to β-sheet (*34, 46*). Turns and amino acid side-chain contributions can also be observed in the 1660−1690 cm^{-1} region (*34, 46*).

The appearance of spectral frequencies that are typically assigned to β-strands could be due to an intramolecular conformational rearrangement of the dimerized or trimerized protein in detergent micelles (*43*). However, given the increased aggregation observed in these samples, prepared without hydroxyapatite chromatography (Figure 3), we favor the attribution of these spectral changes to the introduction of intermolecular hydrogen bonds (*81*). Thermally denatured protein may be able to make stronger intermolecular hydrogen bonds, resulting in spectral components at yet lower frequencies (*81*), because of increased exposure of hydrophobic regions of the protein in the thermally denatured state.

We also performed FT-IR studies on proteoliposomes containing lactose permease. With these studies, we also addressed the differences between our FT-IR results on monomeric lactose permease and the findings of ref *86*. Our spectra on proteoliposomes containing functional lactose permease are similar to those of ref *86*. Amide I and II bands are observed at 1655 and 1544 cm^{-1} in 5 mM TES, pH 8.0. The amide I band, exhibits an additional shoulder at 1635 cm^{-1}. Upon deuterium exchange, the amide I′ band shifts to 1650 cm^{-1}, and the amide II band decreases dramatically in intensity. The shoulder at 1635 cm^{-1} is unaffected by this treatment. Spectral features attributed to lipid vibrational modes are also observed at 1739, 1645, and 1467 cm^{-1}. The 1645 cm^{-1} feature overlaps the protein's amide I band.

To make an accurate secondary structure assignment by analysis of the amide I band, it is important that the lipid contribution in this region be accurately and completely subtracted from the proteoliposome spectrum. In our attempts to carry out this subtraction, we found that the spectral features assignable to lipids shift slightly in frequency and line shape upon protein reconstitution into the liposomes. These changes may be a result of lipid−protein interactions occurring in the bilayer. These effects prevented interpretation of the amide I line shape of lactose permease reconstituted into proteoliposomes.

Regardless of our inability to obtain detailed secondary structure information from proteoliposomes, we do see significant differences in the amide I line shape when these samples are compared to data obtained from monodisperse lactose permease samples. There are several possible explanations for the difference in amide I line shape observed. We favor the explanation that all or a substantial part of the change in amide I line shape is the result of lipid contributions in this spectral region. However, we cannot rule out the possibility that the change is induced by partial dehydration of proteoliposome samples or by reconstitution itself.

Our FT-IR studies also reveal that the purified, monodisperse lactose permease and functional lactose permease reconstituted into proteoliposomes are highly susceptible to isotope exchange when compared to other α-helical membrane proteins, such as photosystem II and bacteriorhodopsin (*43, 70, 71*). This conclusion is supported by the observation that deuterium-exchanged monomeric lactose permease showed a prominent amide II′ band at approximately 1457 cm^{-1} and no detectable amide II band at 1550 cm^{-1}. This conclusion is also supported by the disappearance of the amide II band upon deuterium exchange of proteoliposomes. This result was obtained on monomeric lactose permease at either p^{2}H 8.0 or 5.5, where the rate of base-catalyzed exchange is expected to be over 3 orders of magnitude slower (reviewed in ref *87*). The results of this p^{2}H study indicate that the rate of exchange at high p^{2}H is many orders of magnitude faster than the exchange time. By comparison, photosystem II, which was exchanged for longer periods of time and was in DM micelles at p^{2}H 6.5, showed significantly more intensity in the amide II region. Since the analysis of the amide I line shape for the lactose permease supports the conclusion that the protein has well-defined secondary structure in DM micelles, our results indicate that the α-helical domains of the lactose permease are highly susceptible to ^{2}H exchange. Such susceptibility has also been noted in a separate study of the reconstituted lactose permease (*86*). Moreover, a high degree of ^{2}H exchange has been observed in a pore/channel-forming membrane protein, CHIP28, and a human erythrocyte glucose trans-

porter (*75*, *76*).

There are two possible explanations of facile isotope exchange in proteins. Deuterium exchange can occur either as a result of a cooperative unfolding of the protein or as a result of dynamic fluctuations of the folded state (for discussion, see refs *83* and *87*). To distinguish between these two possibilities, the thermal stability of the monodisperse, monomeric protein in detergent micelles was determined. In addition, estimates of the secondary structure were obtained (see above). Observation of a high denaturation temperature and the high α-helical content of the lactose permease argues against the first possible explanation. Thus, we conclude that, at 20 °C, the monodisperse lactose permease in detergent micelles is stably folded, and we favor the hypothesis that isotope exchange occurs as the result of dynamic fluctuations of the folded state.

This type of facile ^{2}H exchange is consistent with increased conformational flexibility in lactose permease when compared to photosystem II and bacteriorhodopsin. Such flexibility may be due to the presence of a relatively isoenergetic set of available, static folded structures or to a time domain-based averaging over a variety of conformational states. This flexibility may be mechanistically important. For example, conformational flexibility has also been suggested to be involved in the mechanism of glucose transport by the human erythrocyte glucose transporter, which, like lactose permease, has been found to be highly susceptible to ^{2}H exchange (*76*). Recent functional models of the lactose permease suggest that large changes in tertiary structure occur during transport (*23*). Thus, the spectroscopic data presented here are consistent with our model for the structure and function of the lactose permease (*23*).

ACKNOWLEDGMENT

We thank Dr. R. Hutchison for providing a spectrum of PSII and for assistance with spectral curve fitting. We also thank Dr. Hutchison and Professor C. Woodward for helpful discussions. Amino acid composition analysis and N-terminal sequencing were performed by the University of Minnesota Microchemical Facility.

REFERENCES

1. Konings, W. N., Kaback, H. R., and Lolkema, J. S. (1996) *Handbook of Biophysics: Transport Processes in Eukaryotic and Prokaryotic Organisms*, Elsevier, Amsterdam.
2. Marger, M. D., and Saier, M. H., Jr. (1993) *Trends Biochem. Sci. 18*, 13−20.
3. Dinh, T., Paulsen, I. T., and Saier, M. H., Jr. (1994) *J. Bacteriol. 176*, 3825−3831.
4. Pao, S. S., Paulsen, I. T., and Saier, M. H., Jr. (1998) *Microbiol. Mol. Biol. Rev. 62*, 1−34.
5. Varela, M. F., and Wilson, T. H. (1996) *Biochim. Biophys. Acta 1276*, 21−34.
6. West, I. C., and Mitchell, P. (1973) *Biochem. J. 132*, 587−592.
7. Mitchell, P. (1963) *Biochem. Soc. Symp. 22*, 142−168.
8. Teather, R. M., Müller-Hill, B., Abrutsch, U., Aichele, G., and Overath, P. (1978) *Mol. Gen. Genet. 159*, 239−248.
9. Büchel, D. E., Gronenborn, B., and Müller-Hill, B. (1980) *Nature 283*, 541−545.
10. Foster, D. L., Boublik, M., and Kaback, H. R. (1983) *J. Biol. Chem. 258*, 31−34.
11. Calamia, J., and Manoil, C. (1990) *Proc. Natl. Acad. Sci. U.S.A. 87*, 4937−4941.
12. Mieschendahl, M., Büchel, D., Bocklage, H., and Müller-Hill, B. (1981) *Proc. Natl. Acad. Sci. U.S.A. 78*, 7652−7656.
13. Page, M. G. P., and Rosenbusch, J. P. (1988) *J. Biol. Chem. 263*, 15906−15914.
14. Sun, J., Wu, J., Carrasco, N., and Kaback, H. R. (1996) *Biochemistry 35*, 990- 998.
15. Herzlinger, D., Viitanen, P., Carrasco, N., and Kaback, H. R. (1984) *Biochemistry 23*, 3688−3693.
16. Carrasco, N., Tahara, S. M., Patel, L., Goldkorn, T., and Kaback, H. R. (1982) *Proc. Natl. Acad. Sci. U.S.A. 79*, 6894−6898.
17. Brooker, R. J., Fiebig, K., and Wilson, T. H. (1985) *J. Biol. Chem. 260*, 16181−16186.
18. Brooker, R. J., and Wilson, T. H. (1985) *Proc. Natl. Acad. Sci. U.S.A. 82*, 3959−3963.
19. Brooker, R. J. (1990) *J. Biol. Chem. 265*, 4155−4160.
20. Franco, P. J., and Brooker, R. J. (1991) *J. Biol. Chem. 266*, 6693−6699.
21. Franco, P. J., and Brooker, R. J. (1994) *J. Biol. Chem. 269*, 7379−7386.
22. Matzke, E. A., Stephenson, L. J., and Brooker, R. J. (1992) *J. Biol. Chem. 267*, 19095−19100.
23. Jessen-Marshall, A. E., and Brooker, R. J. (1996) *J. Biol. Chem. 271*, 1400- 1404.
24. Kaback, H. R. (1996) in *Handbook of Biological Physics: Transport Processes in Eukaryotic and Prokaryotic Organisms* (Konings, W. N., Kaback, H. R., and Lolkema, J. S., Eds) pp 203−227, Elsevier, Amsterdam.
25. Goswitz, V. C., and Brooker, R. J. (1995) *Protein Sci. 4*, 534−537.
26. Voss, J., Salwiñski, L., Kaback, H. R., and Hubbell, W. L. (1995) *Proc. Natl. Acad. Sci. U.S.A. 92*, 12295−12299.
27. Voss, J., Hubbell, W. L., and Kaback, H. R. (1995) *Proc. Natl. Acad. Sci. U.S.A. 92*, 12300−12303.
28. Jung, K., Voss, J., He, M., Hubbell, W. L., and Kaback, H. R. (1995) *Biochemistry 34*, 6272−6277.
29. He, M. M., Voss, J., Hubbell, W. L., and Kaback, H. R. (1995) *Biochemistry 34*, 15661−15666.
30. He, M. M., Voss, J., Hubbell, W. L., and Kaback, H. R. (1995) *Biochemistry 34*, 15667−15670.
31. Jung, K., Jung, H., Wu, J., PrivÇ, G. G., and Kaback, H. R. (1993) *Biochemistry 32*, 12273−12278.
32. Jung, K., Jung, H., and Kaback, H. R. (1994) *Biochemistry 33*, 3980−3985.
33. Jackson, M., and Mantsch, H. H. (1995) *Crit. Rev. Biochem. Mol. Biol. 30*, 95- 120.
34. Surewicz, W. K., Mantsch, H. A., and Chapman, D. (1993) *Biochemistry 32*, 389−394.
35. Perrin, D. D., and Armarego, W. L. F. (1989) *Purification of Laboratory Chemicals*, p 211, Pergamon Press, Oxford, England.
36. Teather, R. M., Bramhall, H., Riede, I., Wright, J. K., Furst, M., Aichele, G., Wilhelm, U., and Overath, P. (1980) *Eur. J. Biochem. 108*, 223−231.
37. Bradford, M. M. (1976) *Anal. Biochem. 72*, 248−254.
38. Laemmli, U. K. (1970) *Nature 227*, 680−685.
39. Ausubel, F. M. (1992) in *Short Protocols in Molecular Biology* (Ausubel, F. M., Brent, R., Kingston, R. E., Moore, D. D., Seidman, J. G., Smith, J. A., and Struhl, K., Eds.) pp 1028−1030, John Wiley & Sons, New York.
40. Blake, M. S., Johnston, K. H., Russell-Jones, G. J., and Gotschlich, E. C. (1984) *Anal. Biochem. 136*, 175−179.
41. Moore, S., and Stein, W. H. (1963) *Methods Enzymol. 6*, 819−831.
42. Fersht, A. (1977) *Enzyme Structure and Mechanism*, p 170, W. H. Freeman and Co., New York.
43. Hutchison, R. S., Betts, S. D., Yocum, C. F., and Barry, B. A. (1998) *Biochemistry 37*, 5643−5653.
44. Kauppinen, J. K., Moffatt, D. J., Mantsch, H. H., and Cameron, D. G. (1981) *Appl. Spectrosc. 35*, 271−276.
45. Eckert, K., Grosse, R., Malur, J., and Repke, K. R. H. (1977) *Biopolymers 16*, 2549−2563.
46. Susi, H., and Byler, D. M. (1986) *Methods Enzymol. 130*, 290−311.

47. Pourcher, T., Leclercq, S., Brandolin, G., and Leblanc, G. (1995) *Biochemistry 34*, 4412−4420.
48. Pos, K. M., Bott, M., and Dimroth, P. (1994) *FEBS Lett. 347*, 37−41.
49. Stüber, D., Matile, H., and Garotta, G. (1990) *Immunol. Methods 4*, 121−152.
50. Waeber, U., Buhr, A., Schunk, T., and Erni, B. (1993) *FEBS Lett. 324*, 109−112.
51. Crowe, J., Dobeli, H., Gentz, R., Hochuli, E., Stüber, D., and Henco, K. (1994) *Methods Mol. Biol. 31*, 371−387.
52. Mukhija, S., and Erni, B. (1996) *J. Biol. Chem. 271*, 14819−14824.
53. Newman, M. J., Foster, D. L., Wilson, T. H., and Kaback, H. R. (1981) *J. Biol. Chem. 255*, 11804−11808.
54. Hosler, J. P., Fetter, J., Tecklenberg, M. M. J., Espe, M., Lerma, C., and Ferguson-Miller, S. (1992) *J. Biol. Chem. 267*, 24264−24272.
55. Creighton, T. E. (1993) *Protein Structure and Molecular Properties*, pp 28−31, W. H. Freeman & Co., New York.
56. Rigaud, J., Pitard, B., and Levy, D. (1995) *Biochim. Biophys. Acta 1231*, 223−246.
57. Racker, E. (1979) *Methods Enzymol. 55*, 699−711.
58. Zakim, D., and Scotto, A. W. (1989) *Methods Enzymol. 171*, 253−274.
59. Casey, R. P. (1984) *Biochim. Biophys. Acta 768*, 319−347.
60. Eytan, G. D. (1982) *Biochim. Biophys. Acta 694*, 185−202.
61. VanAken, T., Foxall-VanAken, S., Castleman, S., and Ferguson-Miller, S. (1986) *Methods Enzymol. 125*, 27−35.
62. MacDonald, G. M., and Barry, B. A. (1992) *Biochemistry 31*, 9848−9856.
63. Noren, G. H., Boerner, R. J., and Barry, B. A. (1991) *Biochemistry 30*, 3943- 3950.
64. Bentaboulet, M., and Kepes, A. (1977) *Biochim. Biophys. Acta 471*, 125−134.
65. Wong, P. T. S., and Wilson, T. H. (1970) *Biochim. Biophys. Acta 196*, 336−344.
66. Kaczorowski, G. J., Robertson, D. E., and Kaback, H. R. (1979) *Biochemistry 18*, 3697−3704.
67. Heytler, P. G. (1980) *Methods Enzymol. 55*, 442−462.
68. Krimm, S., and Bandekar, J. (1986) in *Advances in Protein Chemistry* (Anfinsen, C. B., Edsall, J. T., and Richards, F., Eds.) pp 181−364, Academic Press, New York.
69. Byler, D. M., and Susi, H. (1986) *Biopolymers 25*, 469−487.
70. Earnest, T. N., Herzfeld, J., and Rothschild, K. J. (1990) *Biophys. J. 58*, 1539- 1546.
71. Bernard, M. T., MacDonald, G. M., Nguyen, A. P., Debus, R. J., and Barry, B. A. (1995) *J. Biol. Chem. 270*, 1589−1594.
72. Luo, S., Huang, C. F., McClelland, J. F., and Graves, D. J. (1994) *Anal. Biochem. 216*, 67−76.
73. Susi, H., and Byler, D. M. (1983) *Biochem. Biophys. Res. Commun. 115*, 391−397.
74. Haris, P. I., Ramesh, B., Sansom, M. S. P., Kerr, I. D., Srai, K. S., and Chapman, D. (1994) *Protein Eng. 7*, 255−262.
75. Haris, P. I., Chapman, D., and Benga, G. (1995) *Eur. J. Biochem 233*, 659−664.
76. Alvarez, J., Lee, D. C., Baldwin, S. A., and Chapman, D. (1987) *J. Biol. Chem. 262*, 3502−3509.
77. Dong, A., Huang, P., and Caughey, W. S. (1990) *Biochemistry 29*, 3303−3308.
78. Holloway, P. W., and Mantsch, H. H. (1989) *Biochemistry 28*, 931−935.
79. Prestrelski, S. J., Byler, D. M., and Thompson, M. P. (1991) *Int. J. Pept. Protein Res. 37*, 508−512.
80. Wolkers, W. F., Haris, P. I., Pistorius, A. M. A., Chapman, D., and Hemminga, M. A. (1995) *Biochemistry 34*, 7825−7833.
81. Clark, A. H., Saunderson, D. H. P., and Suggett, A. (1981) *Int. J. Pept. Protein Res. 17*, 353−364.
82. Surewicz, W. K., and Mantsch, H. H. (1988) *Biochim. Biophys. Acta 952*, 115−130.
83. Dong, A., Hyslop, R. M., and Pringle, D. L. (1996) *Arch. Biochem. Biophys. 333*, 275−281.
84. Heimburg, T., Esmann, M., and Marsh, D. (1997) *J. Biol. Chem. 272*, 25685- 25692.
85. Vogel, H., Wright, J. K., and Jähnig, F. (1985) *EMBO J. 4*, 3625−3631.
86. Le Coutre, J., Narasimhan, L. R., Patel, C. K. N., and Kaback, H. R. (1997) *Proc. Natl. Acad. Sci. U.S.A. 94*, 10167−10171.
87. Woodward, C. K. (1994) *Curr. Opin. Struct. Biol. 4*, 112−116.

BI981142X